COMMUNICATION

Check for updates

Extending the Hammett correlation to mechanochemical reactions†

Leonarda Vugrin,‡[a] Maria Carta,‡[b] Francesco Delogu [iD] *[b] and Ivan Halasz [iD] *[a]

Using Raman *in situ* monitoring and mechanochemistry-specific kinetic analysis, we find a correlation between the reaction probability and the Hammett constants in a model mechanochemical reaction of imine formation, indicating that the body of knowledge developed in physical–organic chemistry could be transferable to ball milling reactions in the solid state.

The Hammett correlation is a remarkable success in organic chemistry, where it has served as a major tool in deciphering the mechanisms of organic reactions, and still remains the subject of recent research.[1–5] Here, we were curious whether the Hammett correlation might hold if solvation is taken out of the picture and the reactions are conducted by mechanochemical ball milling in the solid state, where the reacting molecules are in a different environment as compared to solution.[6–8] The Hammett correlation was recently found in single-molecule mechanochemical bond breaking,[9] while experimental and theoretical modelling indicated facile molecular mobility in the solid state,[10,11] and energetic studies supported solution-like features of milling reactions.[12]
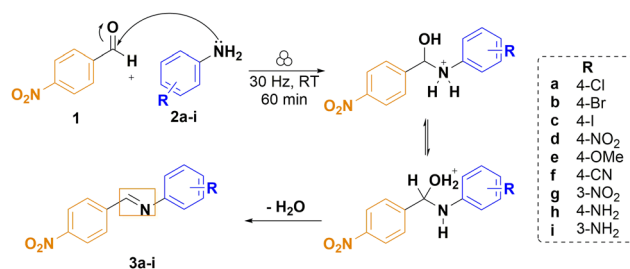
Our interest in the topic emerges from the recent recognition of mechanochemical milling reactions as a viable and valuable synthesis tool,[13,14] but with sparsely rationalised reaction mechanisms. If applicable to mechanochemical milling reactions, the Hammett correlation will provide further mechanistic support for understanding and planning in this increasingly important synthetic methodology.

As a model system to test the validity of the Hammett correlation, we focused on imine (*i.e.* a Schiff base or an azomethine) formation from aromatic aldehydes and anilines.[15,16] Since more than a few substituted benzaldehydes and anilines are low-melting

[a] Ruđer Bošković Institute, Bijenička c. 54, Zagreb 10000, Croatia. E-mail: ivan.halasz@irb.hr

[b] Department of Mechanical, Chemical and Materials Engineering, University of Cagliari, via Marengo 2, Cagliari 09123, Italy. E-mail: francesco.delogu@unica.it

† Electronic supplementary information (ESI) available. See DOI: https://doi.org/10.1039/d2cc06487a

‡ Equal contribution.

soft solids, which could result in pasty and sticky reaction mixtures during ball milling, we limited this study to high-melting point aldehydes and anilines. Specifically, we chose 4-nitrobenzaldehyde (**1**, melting point 104.5 °C) as the aldehyde and reacted it with a series of anilines (**2a–i**) (Scheme 1 and Table 1). Thus, an appropriate equimolar quantity of each aryl amine and (**1**) was milled at room temperature in translucent poly(methyl)methacrylate jars at 30 Hz on a vibratory ball mill and the reaction course was monitored by *in situ* Raman spectroscopy (Scheme 1 and Fig. S3–S10, ESI†).[17]

The imine forming reactions were conducted by neat grinding and provided the target imines (**3a–3i**), or their hydrates,[15] as yellow solids. Some imines were obtained pure after as little as 5 minutes of milling, while 60 minutes was sufficient to have all the reactions run to completion, except for the reaction with 4-nitroaniline, which did not provide the imine by neat grinding (Table 1). Attempts to catalyse this reaction, where both reactants bear an electron-withdrawing *p*-nitro group, will be reported elsewhere.[18] We have also avoided anilines with functional groups that might participate in any hydrogen transfer reactions, such as the hydroxyl-substituted anilines.

The reaction between the benzaldehyde and the aniline is a nucleophilic attack of the aniline amino group on the carbon atom of the aldehyde moiety followed by an elimination reaction leading to the formation of a C=N double bond and the

Scheme 1 Neat grinding reaction of imine formation from (**1**) and substituted anilines (**2a–i**) and the proposed reaction mechanism in solution.[16]

Table 1 Substituted aryl amines, their properties and reaction outcomes

Entry	Aryl amine	R	m.p. (°C)	σ	NMR yield[a] (%)
1	**2a**	4-Cl	69.5	0.23	98
2	**2b**	4-Br	59.0	0.23	98
3	**2c**	4-I	62.0	0.18	100
4	**2d**	4-NO$_2$	147.5	0.78	NR[b]
5	**2e**	4-CN	84.0	0.66	97
6	**2f**	4-OMe	57.5	−0.27	99
7	**2g**	3-NO$_2$	114.0	0.71	98[c]
8	**2h**	4-NH$_2$	143.5	−0.66	100

[a] After 60 minutes of milling. [b] No reaction. [c] NMR yield after milling for 2 h.

final imine (Scheme 1).[16] In solution, it is known that the imine formation is acid- or base-catalysed with a proposed reaction mechanism that involves hydrogen transfer. For example, in milling (**1**) with (**2a**) we observed the consumption of the starting materials after *ca.* 10 min of milling, which is evidenced by the loss of intensity of the Raman band at 1690 cm^{-1} belonging to the carbonyl group stretching vibration and by the emergence of a new set of bands at around 1600 cm^{-1}, corresponding to the formation of the imine (Fig. 1). Solution NMR of the products and, if possible, Rietveld analysis of the powder diffraction patterns of the obtained solids confirmed the formation of the expected imines (Fig. S12–S24, ESI†).

The reaction profiles were obtained by fitting the intensity of the strongest imine band from the collected time-resolved Raman spectra. The obtained reaction profiles were scaled to

lie in the range [0,1]. All kinetic profiles exhibited the same sigmoidal shape, although the details changed from one substituent to another (Fig. 2). From Fig. 2, the following decreasing trend in the reaction rates is observed: (**3f**) > (**3c**) > (**3b**) > (**3a**) > (**3e**) > (**3h**). The reaction with (**2h**) was the slowest, even though it could have been expected to be the fastest, based on the σ constant for the *p*-NH$_2$ group (Table 1).

The kinetic model that describes the kinetic curve shape is based on quantities that correspond to the reactant interface area and the rate of its generation, the reaction probability, and the volume fraction of the powder in which the reaction conditions are fulfilled.[20,21] In short, we assume that the mechanochemical reaction is governed by:

1. The statistical factor, which is measured by *k*, *i.e.* the volume fraction of powder undergoing critical loading conditions (CLCs) during individual impacts accounts for the stochastic involvement of the powder in impacts during the mechanical processing. Specifically, *k* increases as the slope of the kinetic curve increases.

2. The mechanical or rheological factor, which is measured by *r*, *i.e.* the rate at which the interface between reactants is generated in volumes affected by CLCs and accounts for the forced mixing processes occurring on increasingly smaller length scales. Smaller *r* values result in harder solids, whereas higher *r* values are associated with softer solids.

3. The chemical factor, which is measured by *Π*, *i.e.* the reaction probability between two reactant molecules that are in
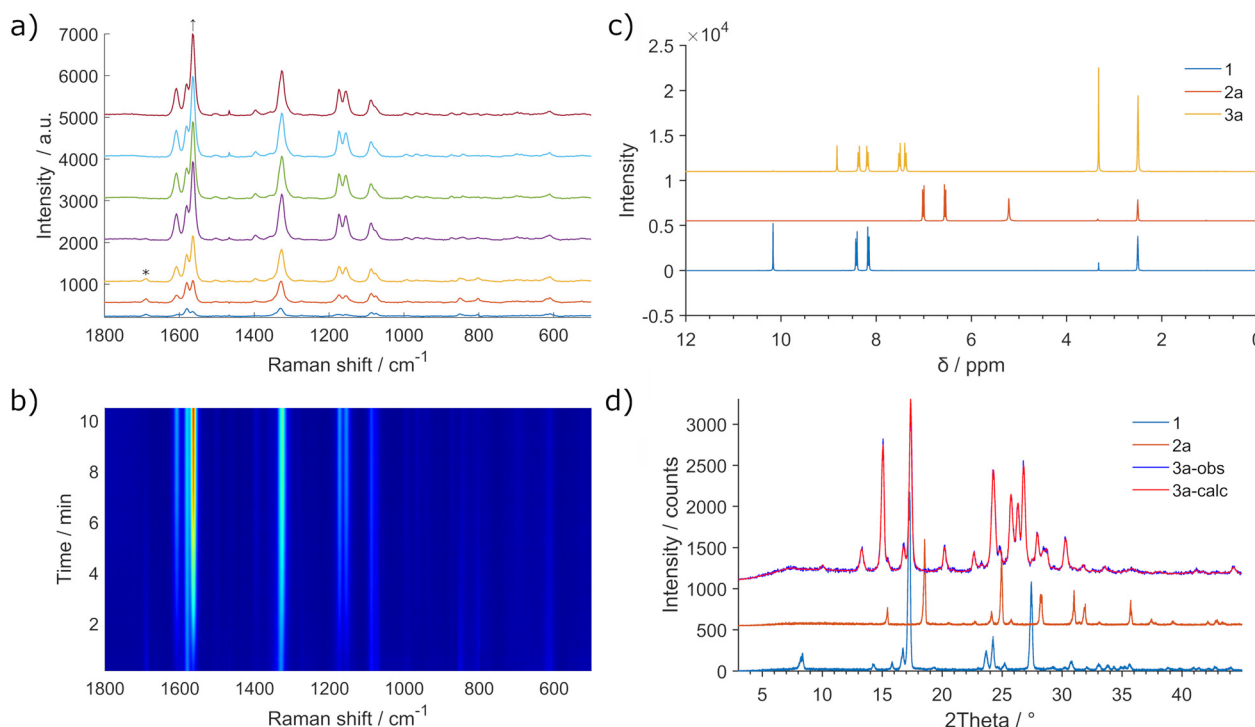
Fig. 1 Mechanochemical imine formation from (**1**) and (**2a**). (a) Selected Raman spectra during 60 min of milling. (b) Time-resolved 2D plot of the neat grinding of an equimolar mixture of (**1**) and (**2a**). The first 10 min of the reaction are shown for a more detailed examination of the changes in the Raman band intensities. Identification of the imine product by (c) solution ^{1}H NMR (DMSO) and (d) Rietveld analysis of the powder X-ray diffraction pattern using the solved crystal structure (CSD refcode UGESOR[19]).
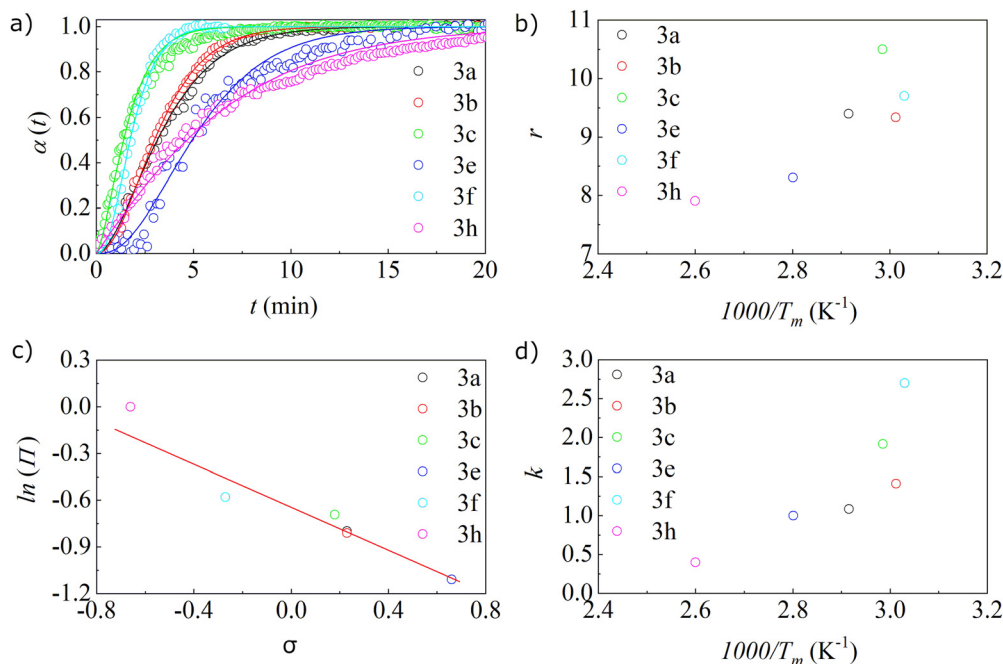
Fig. 2 (a) Global molar fraction $\alpha(t)$ as a function of milling time (t), (b) interface generation rate r as a function of reciprocal of temperature, (c) semi-logarithmic plot of reaction probability at interface as a function of Hammett substituent constants, and (d) volume fraction of powder undergoing CLCs as a function of reciprocal of temperature.

contact at the interface or in a mixed volume accounts for all the thermodynamic and kinetic quantities typically involved in a chemical reaction.

Therefore, our best-fitted curves have the same general equation but differ in the k, r and Π values. We obtained several fitting parameters and observed the existence of different local minima on the surface that described the fitting performance in the fitting parameter space. However, once we assume that reactants can get progressively mixed up to the molecular scale, *i.e.* the initial and final interface areas are approximately the same for all the different cases, our kinetic analysis is compatible with a reaction probability Π dominated by the Hammett factor, denoted with σ. Concerning the Hammett factors, the simple kinetic model provides estimates of the reaction probability at the interface that are consistent with a classical Hammett correlation. Namely, the factor that indicates the volume fraction that experiences CLCs is inversely proportional to the temperature and has the same trend as the previously mentioned dependence of the global molar fraction on the duration of the reaction, *i.e.* the number of impacts: (**3f**) > (**3c**) > (**3b**) > (**3a**) > (**3e**) > (**3h**). In contrast, the rheological factor that describes the rate of generation of the active surface exhibited the following trend: (**3c**) > (**3f**) > (**3a**) > (**3b**) > (**3e**) > (**3h**). The above points to the sensitivity of the statistical and rheological parameters to several factors, such as the hardness and density of the resulting material, which affect the elasticity of the collisions and the different course of the reaction. Namely, if the resulting material is denser, it will lead to a reduction in the volume that can be subjected to further CLCs, causing a slower reaction.

The statistical and mechanical, or rheological, quantities k and r, respectively, are seemingly related and correlated with the inverse of the lower melting point of the two reactants forming the initial mixture (Fig. 2). The lower the melting point, the softer the crystal is. This means that flow deformation can be induced more effectively and mixing can be faster. We have been able to satisfactorily best fit (**3h**) only assuming that the initial interface area was larger than in other cases. This suggests the possible role of water liberated during imine formation. 1,4-Phenylendiamine is, indeed, quite soluble in water, while the other anilines are insoluble or much less soluble. Since imine formation involves the release of water, this could help explain the fact that our fitting suggests that for the reaction between (**2h**) and (**1**), the initial contact area, which measures the propensity to form an interface, is significantly larger than those for other cases. Moreover, this could explain the greater propensity of this reaction mixture to stick to the reaction vessel walls.

The reaction probability Π depends on the orientation of the molecules where the proper orientation gives rise to the chemical reaction. The reaction rate increases as the reaction probability increases. A semi-logarithmic plot of the reaction probability and Hammett parameter is linear with a negative slope, which points to slower reaction when electron-withdrawing substituents on the aniline partners are used. Moreover, the linear dependence of the reaction probability on the Hammett constants indicates that the values of constants of substituents derived for solution result in a similar trend also in the solid state. Remarkably, Π was equal to 1 for the formation of (**3h**). That is, it was almost twice the value

expected for the amino group based on its Hammett σ coefficient (Table 1). Indeed, Π measures the reaction probability and (**2h**) has two equivalent amino groups.

In summary, it may be gratifying to learn that mechanochemistry is not only a mix of exotic energy landscapes and unusual products,[22] but also old chemistry based on the reactivity of functional groups and fundamental concepts of acids and bases,[23] where, more often than not, mechanical work serves primarily to mix the chemical species. Mechanochemical processing is inherently solvent-free and enables reactions between insoluble and immiscible compounds, but the underlying (mechano)chemistry seems to be governed by the common solution-based laws of chemical reactivity. In the case presented here, the imine formation is sensitive to the nucleophilicity of the attacking amino group, expressed by the substituent Hammett constant. Similar systematics based on linear free-energy relationships for mechanochemical reactions using liquid additives are currently under investigation by our groups.

Conflicts of interest

There are no conflicts to declare.

Notes and references

1 L. P. Hammett, *J. Am. Chem. Soc.*, 1937, **59**, 96–103.
2 L. P. Hammett, *Chem. Rev.*, 1935, **17**, 125–136.
3 A. B. Flynn and W. W. Ogilvie, *J. Chem. Educ.*, 2015, **92**, 803–810.
4 M. Bragato, G. F. von Rudorff and O. A. von Lilienfeld, *Chem. Sci.*, 2020, **11**, 11859–11868.
5 H. H. Jaffé, *Chem. Rev.*, 1953, **53**, 191–261.
6 J.-L. Do and T. Friščić, *ACS Cent. Sci.*, 2017, **3**, 13–19.
7 K. Tanaka and F. Toda, *Chem. Rev.*, 2000, **100**, 1025–1074.
8 S. Lukin, L. S. Germann, T. Friščić and I. Halasz, *Acc. Chem. Res.*, 2022, **55**, 1262–1277.
9 M. H. Barbee, T. Kouznetsova, S. L. Barrett, G. R. Gossweiler, Y. Lin, S. K. Rastogi, W. J. Brittain and S. L. Craig, *J. Am. Chem. Soc.*, 2018, **140**, 12746–12750.
10 S. Lukin, M. Tireli, T. Stolar, D. Barišić, M. V. Blanco, M. di Michiel, K. Užarević and I. Halasz, *J. Am. Chem. Soc.*, 2019, **141**, 1212–1216.
11 M. Ferguson, M. S. Moyano, G. A. Tribello, D. E. Crawford, E. M. Bringa, S. L. James, J. Kohanoff and M. G. D. Pópolo, *Chem. Sci.*, 2019, **10**, 2924–2929.
12 J. M. Andersen and J. Mack, *Chem. Sci.*, 2017, **8**, 5447–5453.
13 J. L. Howard, Q. Cao and D. L. Browne, *Chem. Sci.*, 2018, **9**, 3080–3094.
14 T. Friščić, C. Mottillo and H. M. Titi, *Angew. Chem., Int. Ed.*, 2020, **59**, 1018–1029.
15 J. Schmeyers, F. Toda, J. Boy and G. Kaupp, *J. Chem. Soc., Perkin Trans. 2*, 1998, 989–994.
16 E. H. Cordes and W. P. Jencks, *J. Am. Chem. Soc.*, 1962, **84**, 832–837.
17 S. Lukin, K. Užarević and I. Halasz, *Nat. Protoc.*, 2021, **16**, 3492–3521.
18 L. Vugrin, I. Cvrtila, M. Juribašić Kulcsár and I. Halasz, *Croat. Chem. Acta*, 2023, submitted.
19 S. Leela, A. Subashini, P. Reji, K. Ramamurthi and H. Stoeckli-Evans, *Acta Crystallogr., Sect. E: Crystallogr. Commun.*, 2020, **76**, 417–422.
20 M. Carta, F. Delogu and A. Porcheddu, *Phys. Chem. Chem. Phys.*, 2021, **23**, 14178–14194.
21 G. Traversari, A. Porcheddu, G. Pia, F. Delogu and A. Cincotti, *Phys. Chem. Chem. Phys.*, 2021, **23**, 229–245.
22 J. Andersen and J. Mack, *Green Chem.*, 2018, **20**, 1435–1443.
23 M. Sander, S. Fabig and L. Borchardt, *Chem. – Eur. J.*, 2022, e202202860.